Photoemission from activated gallium arsenide. II. Spin polarization versus kinetic energy analysis

H.-J. Drouhin, C. Hermann, and G. Lampel
Laboratoire de Physique de la Matière Condensée, Ecole Polytechnique, 91128 Palaiseau, France
(Received 17 July 1984)

The spin polarization of the electrons emitted by a GaAs photocathode under circularly polarized light excitation is investigated as a function of the electron kinetic energy. The photocathode is activated by cesium and oxygen coadsorption under ultrahigh-vacuum conditions to achieve a negative electron affinity. The spin polarization is measured by Mott scattering. The study is performed with a very-high-energy resolution (20 meV), at 300 and 120 K, under well-focused Kr^+-laser light excitation (photon energy ranging from 1.55 to 2.60 eV). The polarization-versus-energy distribution curves show typical features related to those observed in the energy distribution curves, which are analyzed in detail in the preceding paper [H.-J. Drouhin, C. Hermann, and G. Lampel, Phys. Rev. B **31**, 3859 (1985)]. A model is developed to account for the largest measured polarization, which arises from electrons excited from the heavy-hole band and emitted without suffering any collision: A $\frac{2}{3}$ maximum value is expected, which is reduced by spin precession in the internal D'yakonov and Perel' (DP) field, due to the absence of space-inversion symmetry in GaAs. An estimation of the hot-electron mean free path (~ 0.1 μm for photon energy above 1.96 eV) is deduced. The photoemission polarizations of the electrons excited from each of the two other valence bands are also calculated using a nonparabolic Kane band model. The L and X subsidiary minima give rise to polarization plateaus originating from energy relaxation in the band-bending region. The main contribution to the photocurrent is due to electrons which were thermalized in the central minimum of the bulk crystal and have relaxed their energy in the band-bending region prior to emission into vacuum. Their polarization is studied in relation with the luminescence polarization, measured on the same samples, in the framework of a one-dimensional diffusion model. An additional depolarization, occurring during the escape process, is evidenced and attributed to the DP relaxation mechanism in the band-bending region. Finally, the performances of GaAs photocathodes as monochromatic and polarized electron sources are analyzed with use of the physical concepts developed in the present paper and in the preceding one.

I. INTRODUCTION

In gallium arsenide, absorption of circularly polarized light of energy slightly greater than the band gap gives rise to a spin-polarized electron population in the conduction band: This is the so-called optical pumping of conduction electrons.[1,2]

The work function of heavily doped p-type GaAs can be sufficiently lowered to achieve a negative electron affinity (NEA).[3] Therefore, GaAs photocathodes have been used to implement very-high-efficiency photoemitters.[4] In optical-pumping conditions, they also proved to be convenient spin-polarized electron sources.[5,6] Although such sources are now widely used, only little understanding of the physics of spin-polarized NEA photoemission has been achieved up to now. To elucidate the fundamental polarization properties relevant to NEA GaAs photocathodes, we relate the degree of spin orientation of the photoemitted electrons to their kinetic energy.

In the preceding paper[7] (hereafter referred to as I), we have presented an extensive study of the energy distribution curves (EDC's) of the electrons emitted from a NEA GaAs photocathode: After photoexcitation into the conduction band, the electrons relax their energy; a fraction of them is emitted during the thermalization process and gives rise to characteristic features in the EDC's. The hot-electron structures, corresponding to the final states of the optical transitions, were interpreted with the use of nonparabolic-band $\vec{k}\cdot\vec{p}$ perturbation model. The essential role played by the subsidiary conduction minima in the energy relaxation and photoemission processes was emphasized. We confirmed that the major part of the photoemitted current originates from electrons thermalized at the Γ minimum of the conduction band in the solid, and relaxed in the band-bending region prior to emission.[8]

In this paper (hereafter referred to as II), we analyze the polarization of the photoemitted electrons as a function of their kinetic energy. Preliminary results were reported in Refs. 9 and 10. Polarization of the bulk electrons was already studied through thermalized[1] and hot photoluminescence.[11] The importance of spin relaxation was evidenced and several spin-relaxation mechanisms were proposed and discussed.[12,13] However, if luminescence measurements probe the electron polarization inside the solid, the photoemission experiments also permit the study of the escape process through the band-bending region and yield detailed information on the spin relaxation during the energy-loss steps.[9,14]

In the following sections, we first describe the experiment (Sec. II); we then recall the theoretical background

on electron spin polarization in bulk GaAs and on activated GaAs photoemission (Sec. III). In Sec. IV we investigate the degree of spin orientation of the photoemitted electrons as a function of their kinetic energy. Nonthermalized electron effects and the importance of hot-electron spin relaxation are emphasized. The influence of the band-bending region on the polarization of the thermalized photoemission is evidenced. A comparison is made between the electron polarization in the bulk crystal, measured in thermalized and hot-luminescence experiments, and in vacuum. The last part of the paper (Sec. V) applies the results obtained in the preceding sections, as well as in I, to NEA GaAs photocathodes: we showed in a previous paper[9] that they provide not only polarized but also very intense monochromatic electron beams.

II. EXPERIMENT

The experimental setup is schematized in Fig. 1. The crystal is illuminated normal to its surface by a Kr^+ or He-Ne laser, σ^+ or σ^- circularly polarized through a Babinet-Soleil compensator. The electron spins are oriented along the incident-light direction Oz; with respect to this axis, the polarization P is defined by $P=(n_+ - n_-)/(n_+ + n_-)$, where $n_+(n_-)$ is the number of electrons with spin up (down).

The energy selection system was described in I. Here, we briefly recall its essential features. The photoemitted electrons are energy selected by a cylindrical 90° electrostatic deflector operating in the constant-energy mode. The full width at half maximum (FWHM) of the transmission function is $\Delta E \simeq 20$ meV. In these conditions, the current transmitted through the selector (10^{-3} to 10^{-2} of the total emitted current) may exceed 5 nA without EDC distorsion. EDC derivatives are obtained by

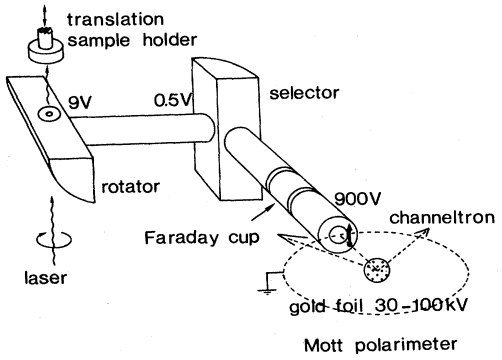

FIG. 1. Schematic diagram of the apparatus. The photocathode, mounted on a translation displacement, is illuminated normal to its surface. The emitted electrons are successively 90° deflected in the rotator, decelerated, and energy analyzed in the selector. The indicated bias voltages correspond to a 20-meV resolution. The electrons can either be collected into the Faraday cup, which provides the EDC, or reaccelerated to the Mott polarimeter, where their spin orientation is measured: There, they are scattered on a gold foil at a high potential and detected by two symmetrical channeltrons. The asymmetry of the counting rates is proportional to the electron polarization. For a circularly polarized laser excitation, the electron spins are oriented along the heavy arrow.

adding a 15-mV peak-to-peak modulation to the photocathode bias voltage.

The polarization of the energy selected electrons is measured by Mott scattering on a gold foil at high voltage V_0. We use a Mott detector with concentric cylindrical electrode geometry described in Ref. 15. It is designed for ultrahigh-vacuum operation and currently used in the 10^{-9}-Torr range while the main chamber is kept at a pressure $<2.10^{-10}$ Torr owing to differential pumping. The spin-dependent asymmetry $A(V_0)=(N_+ - N_-)/(N_+ + N_-)$, measured from the counting rates N_+ and N_- of two channeltrons located at polar angles $\pm 120°$ from the incident beam, is the product of the Sherman function $S(V_0)$ by the polarization component along the normal to the scattering plane. In our experiment, this direction is the spin-orientation axis of the incident electrons (see Fig. 1), so that $A(V_0)=S(V_0)P$. Data acquisition and polarization calculations are performed through a microcomputer. The instrumental asymmetry is eliminated by comparing the polarization values measured under σ^+,σ^- and linearly polarized light excitation. Corrections for multiple and plural scatterings are deduced from the channeltron cone voltage extrapolation which was shown to be equivalent to zero foil thickness extrapolation.[15] The asymmetry $A(V_0)$ is referred to that measured at 100 kV, so that only the knowledge of $S(100$ kV) is required to determine P. There are some discrepancies between the experimental and theoretical values quoted in the literature,[16] and we shall take the most commonly used value, $S(100\text{ kV})=0.39$. We usually operate at $V_0=30$ kV, for which we verified that $S(30\text{ kV})/S(100\text{ kV})=0.82$.[15] This condition maximizes the figure of merit $[S(V_0)]^2R/R_0$, where R is the detected current and R_0 is the current at the entrance of the Mott scatterer.[15] With a 120-nm-thick gold foil, the efficiency R/R_0 is about 10^{-5}. Consequently, the polarization of an electron beam as weak as 1 pA (to be compared to 5 nA, the peak output current of the selector) is measured in 10 min with a statistical error $\sim 10^{-2}/S(V_0)$. The precision is not limited by the background count rate of the detectors which is only of a few counts per min. We are then able to measure spin-polarization variations over very weak structures of the EDC's. Yet, if relative variations of the polarization can be accurately observed, it has been pointed out[17] that systematic effects and uncertainties limit the precision of *absolute* measurements on Mott polarimeters to $\sim 5.10^{-2}P$.

Recently, other techniques have been developed for spin detection, such as low-energy electron diffraction[18,19] or spin-dependent absorption in solids.[20–23] Although very sensitive and of simple use, they nevertheless depend on various parameters (surface preparation, beam energy, scattering angle) and need external calibration. The uncertainties on the absolute value of the polarization are then difficult to estimate. It is important to keep all these limitations in mind when comparing polarization values quoted in the literature.

The results we report here are obtained on two different p-type GaAs samples, doped with zinc ($\sim 10^{19}$ cm^{-3}) and oriented parallel to the (100) plane. We have chosen them for their very different polarized luminescence properties

(see Sec. IV C 2).

Sample 1. Taken from a C-31034 RCA photomultiplier tube.

Sample 2. Commercial M/A-Com Laser Diode Inc. crystal.

These samples are cleaned using the procedure described in I (Refs. 4 and 6) and activated by cesium and oxygen coadsorption (at a pressure in the low 10^{-10}- and 10^{-9}-Torr range, respectively). With no cesium excess (which is our usual experimental condition), the total emitted current decreases with time at a rate $\sim 1\%$ per h (see Sec. V C).

The thermalized and hot-luminescence measurements are performed using a standard luminescence equipment with a 0.75-m double Czerny-Turner Jarrell-Ash spectrometer. The samples are clamped on a copper block which can be cooled by contact with liquid nitrogen.

III. THEORETICAL BACKGROUND

Optical pumping in GaAs has been extensively studied in luminescence experiments and various spin-relaxation mechanisms have been considered. In this section, we first review fundamental symmetry properties which govern photoexcitation of spin-polarized electrons. We recall the consequences of spin relaxation of these electrons during their energy relaxation and also when they are thermalized at the bottom of the conduction band. Finally, we derive some simple relations between the electron polarizations in vacuum and in the bulk crystal.

A. Initial spin orientation

GaAs is a direct-gap semiconductor with zinc-blende symmetry. At the Brillouin-zone center Γ, the lowest conduction band (Γ_6 band) is of Γ_6 symmetry;[24] the upper valence bands consist of two bands of Γ_8 symmetry (corresponding to heavy and light holes and noted, respectively, Γ_{8h} and Γ_{8l}) and a spin-orbit-split band (Γ_7 band) belonging to the Γ_7 representation. In optical-pumping experiments, an electron population with a mean spin along the direction Oz of light propagation and of orientation depending on the light helicity,[1,2] is created in the conduction band by absorption of $\sigma^{\pm}$ polarized light of energy $h\nu$ greater than the band gap E_G ($E_G = 1.42$ eV at 300 K and 1.50 eV at 120 K; all the quoted GaAs data are taken from Blakemore's review, Ref. 25). In the following, we consider σ^- polarized light excitation. Each transition $\Gamma_{8h} \rightarrow \Gamma_6$, $\Gamma_{8l} \rightarrow \Gamma_6$, or $\Gamma_7 \rightarrow \Gamma_6$ creates electrons of respective initial polarizations $P_{8h}(h\nu)$, $P_{8l}(h\nu)$, or $P_7(h\nu)$, which are only related to the symmetry of the crystal. For $h\nu$ close to E_G, only the $\Gamma_{8h} \rightarrow \Gamma_6$ and $\Gamma_{8l} \rightarrow \Gamma_6$ transitions are allowed and they lead to $P_{8h}(E_G) = P_{8l}(E_G) = 0.5$. When $h\nu = E_G + \Delta$ ($\Delta = 0.34$ eV, temperature independent, is the spin-orbit energy splitting), the $\Gamma_7 \rightarrow \Gamma_6$ transition also becomes possible and creates -100% polarized electrons.

With increasing wave vector $\vec{k}$, the energy bands are deeply altered, as can be seen in Fig. 2(a), calculated after second-order $\vec{k} \cdot \vec{p}$ perturbation[26] (see Sec. IV A 2 of I): In particular, the spin-orbit coupling effect diminishes, leading to two parallel light- and heavy-hole bands distant of $\simeq 2\Delta/3$ as soon as the light-hole energy becomes of the order of Δ. The initial polarizations reflect the wave-function modifications. In the same framework we have calculated[27] $P_{8h}(h\nu)$, $P_{8l}(h\nu)$, $P_7(h\nu)$, which are plotted in Fig. 2(b): Note that with increasing $|\vec{k}|$, the polariza-

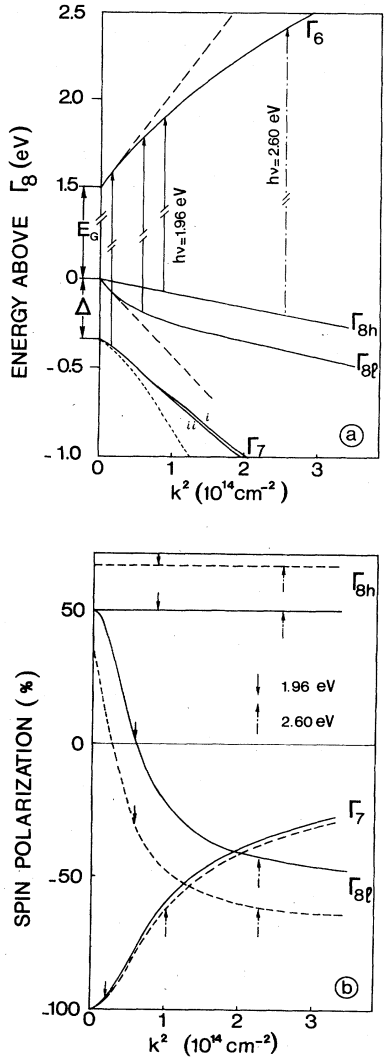

FIG. 2. (a) GaAs band structure around the Brillouin-zone center versus squared wave vector k^2 at 120 K. The solid lines are calculated from the spherical nonparabolic Kane band model (Ref. 26). The three solid vertical arrows schematize the optical transitions by absorption of photons of energy $h\nu = 1.96$ eV. The dot-dashed arrow limits the portion of the Brillouin zone explored in our experiments ($h\nu = 2.60$ eV). For additional comments see the caption of Fig. 8 in I. (b) Polarization versus squared wave vector k^2 at 120 K for the electrons excited from the Γ_{8h}, Γ_{8l}, and Γ_7 bands, calculated using the same band model as in Fig. 2(a) (Ref. 27). The solid curves are angular averaged polarizations, the dashed curves are the maximum possible photoemission polarizations calculated following the procedure developed in Appendix A. The arrows refer to the polarization at promotion by absorption of photons of energy 1.96 eV (solid arrows) and 2.60 eV (dot-dashed arrows).

tion $P_{8l}(h\nu)$ changes its sign, tending to -0.5, whereas $P_7(h\nu)$ decreases to zero and $P_{8h}(h\nu)$ remains unaffected.[28] Consequently, the overall initial polarization, which involves the joint density of states for these three transitions, decreases to zero. We point out that this arises mainly because $P_{8h}(h\nu)$ and $P_{8l}(h\nu)$, of opposite signs, are taken into account with comparable weights.

All of the initial polarizations defined above are averages over the electron momentum directions. In fact, just after excitation, the electron distribution is anisotropic and the spin polarization depends on the angle θ between the electron wave vector $\vec{k}$ (of modulus k) and Oz.[29] For instance, for $\Gamma_{8h}\rightarrow\Gamma_6$ transitions, the spin of the electrons promoted with a wave vector $\vec{k}$ is given by[27,29]

$$\vec{S}(\vec{k})=\frac{\cos\theta}{1+\cos^2\theta}\frac{\vec{k}}{k} . \tag{1}$$

In particular, the electrons promoted with a momentum parallel to the light direction are 100% polarized for this transition.

B. Energy and spin relaxation

1. Energy relaxation

After promotion in the conduction band, the electrons undergo energy relaxation. The various mechanisms are reviewed in I [(ii) of Sec. III B]. Whenever it is energetically possible, the electrons are scattered from the central Γ valley to the side ones (L and X minima lying, respectively, 300 and 460 meV above Γ) at the bottom of which they accumulate. In the Γ valley, the electrons lose their energy either by emission of optical phonons, of narrow dispersion and of energy $\hbar\omega_o$ close to 30 meV, or by collision with heavy holes which are transferred to the light-hole band, a mechanism proposed by D'yakonov, Perel', and Yassievich (DPY).[30]

2. Spin relaxation

During their lifetime in the crystal, the photoelectrons undergo various spin-relaxation mechanisms, discussed in Refs. 12 and 13 and recalled in Sec. III C, and lose part of their initial polarization. This depolarization occurs in a two-step process.

(i) The average polarization $P_0(h\nu)$ of the electrons reaching the bottom of the conduction band is determined by the initial polarizations $P_j(h\nu)$ and the spin relaxation during the thermalization process:

$$P_0(h\nu)=\sum_j n_j(h\nu)[f_j(h\nu)P_j(h\nu)] , \tag{2}$$

where the summation index j refers to the three valence bands, $n_j(h\nu)$ is the relative weight of each transition, and $f_j(h\nu)$ is a reduction factor which accounts for the depolarization during energy relaxation between the promotion energy and the thermalized state.

(ii) At the bottom of the conduction band additional spin relaxation occurs, because of the competing effects of lifetime τ and of spin-relaxation time T_1 of thermalized electrons, so that the thermalized polarization becomes[1,2]

$$P_{\text{therm}}(h\nu)=P_0(h\nu)T_1/(T_1+\tau) . \tag{3}$$

C. Spin-relaxation mechanisms inside the crystal

Polarized photoluminescence experiments in GaAs have evidenced different spin-relaxation mechanisms; their relative efficiency strongly depends on the electron kinetic energy.[12,13]

1. Spin relaxation at notable kinetic energy

At kinetic energies exceeding a few 10^{-1} eV for our hole concentration, the most efficient spin-relaxation process was shown to result from the spin splitting of the conduction band,[26,31] as proposed by D'yakonov and Perel' (DP).[32] This splitting can be described in terms of an internal magnetic field (DP field) around which the spin precesses with the precession vector:[12,32]

$$\vec{\omega}(\vec{k})=\sqrt{2}(ab/\hbar k)B'\vec{h}(\vec{k}) . \tag{4}$$

The coefficients a and b are Kane coefficients[26] for the conduction-band wave function, B' is a parameter arising from the coupling between Γ_6 and the remote bands of Γ_5 symmetry, and $\vec{h}(\vec{k})$ is a vector normal to the wave vector $\vec{k}=(k_x,k_y,k_z)$, of components

$$(k_x(k_y^2-k_z^2), k_y(k_z^2-k_x^2), k_z(k_x^2-k_y^2))$$

with respect to the cubic crystal axes.

Upon scattering, the electron momentum and consequently the orientation of the precession axis are changed. When the electrons relax their momentum much faster than their energy, a spin-relaxation time $\tau_s(\epsilon)$ can be defined at the electron kinetic energy ϵ;[12] moreover, in the "weak collision" limit $\omega(\epsilon)\tau_p \ll 1$, where $\omega^2(\epsilon)$ is the angular average of $|\vec{\omega}(\vec{k})|^2$ and τ_p is the momentum relaxation time, $\tau_s(\epsilon)$ is given by

$$\tau_s(\epsilon)^{-1}=\tfrac{2}{3}\omega^2(\epsilon)\tau_c ,$$

where the correlation time τ_c of the interaction responsible for spin relaxation does not differ much from τ_p.[33] In that case, the depolarization is reduced by efficient momentum relaxation in a way similar to motional narrowing.[34] The frequency $\omega(\epsilon)$ is strongly dependent on the electron kinetic energy. Near the Brillouin-zone center (see Appendix A), $\omega(\epsilon)$ is of the order of $1.10^9[\epsilon\ (\text{meV})]^{3/2}$ rad s^{-1}, as calculated in Ref. 12, or $2.10^9[\epsilon\ (\text{meV})]^{3/2}$ rad s^{-1}, as estimated from polarized luminescence experiments.[35]

2. Spin relaxation of thermalized electrons

For thermalized electrons, the dominant spin-relaxation mechanism in the heavily doped p-type samples[12,13] suited for NEA photocathodes arises from the exchange interaction between electrons and holes, as proposed by Bir, Aronov, and Pikus (BAP).[36] For $T>100$ K, the corresponding spin-relaxation time varies as $T^{-3/2}$.[13]

D. Polarized photoemission

Some of the photoexcited electrons reach the cathode surface and escape into vacuum where their polarization

reflects the electron spin orientation inside the crystal but also the characteristics of the emission process.

1. Polarizations outside and inside the solid

(i) The dominant contribution to the total current emitted by a NEA photocathode originates from the electrons which were relaxed at the bottom of the conduction band in the bulk crystal: Their polarization $P_e(h\nu)$ in vacuum may be related to the thermalized electron polarization inside the solid $P_{\text{therm}}(h\nu)$. Assuming that no additional depolarization occurs in the escape process, Lampel and Eminyan[37] use a one-dimensional diffusion model;[6] in the limit of a large surface recombination velocity, which is relevant for GaAs photocathodes,[38,39] they obtain

$$P_e(h\nu)=P_{\text{therm}}(h\nu)[T_1/(T_1+\tau)]^{-1/2} . \quad (5)$$

Consequently, when $h\nu$ varies, the electron polarization in vacuum remains proportional to that of the thermalized electrons in the crystal. Equation (5) expresses the fact that the electrons which escape into vacuum are less depolarized than those which stay in the thermalized state during their whole lifetime τ. Using Eq. (3), we rewrite Eq. (5) as

$$P_e(h\nu)=P_0(h\nu)[T_1/(T_1+\tau)]^{1/2} . \quad (6)$$

Comparison between Eqs. (3) and (6) clearly shows that the electrons photoemitted from the Γ point and those remaining in the crystal at the Brillouin-zone center have experienced the same spin relaxation before reaching the Γ minimum.

(ii) A sizeable fraction of the photoexcited electrons is emitted prior to thermalization in Γ. In previous papers[9,10] we evidenced the decrease of the spin polarization with decreasing electron kinetic energy and related the polarization structures we observed to those present in the EDC's.

2. Method of analysis

The photoemission polarization is determined first by the polarization in the bulk, and possibly by depolarization during the emission stage. Consequently, the study of the electron polarization in vacuum requires the knowledge of the bulk spin depolarization, which is best studied through polarized photoluminescence.

(i) The circular polarization of the thermalized luminescence is directly proportional to $P_{\text{therm}}(h\nu)$. In particular, the ratio τ/T_1, which governs the depolarization in the thermalized state, is very conveniently obtained by this technique.

(ii) A measurement of characteristic times for hot electrons is more difficult; yet hot-luminescence experiments yield valuable information on the photoexcitation process, and the spin and energy relaxations.[11]

Obviously, in all cases the comparison between photoemission and luminescence polarizations must be performed on the *same* sample and at the same temperature: It should be emphasized that all spin-relaxation properties are generally strongly sample and temperature dependent.

In the following section we present a detailed experimental study of the photoemission polarization of both thermalized and hot electrons, which is carried out in conjunction with a precise energy analysis. A clarification of bulk and surface spin effects is achieved by comparison of photoemission results with thermalized and hot polarized luminescence data.

IV. EXPERIMENTAL RESULTS

A polarization versus energy distribution curve (PEDC) reflects the history of the electron polarization from the promotion energy to the lowest accessible energy level in the band-bending region. The longer the electrons undergo the depolarization mechanisms in the crystal before escaping into vacuum, the smaller the remaining polarization. As the time spent inside the crystal increases with the mean energy loss, the measured polarization decreases with decreasing energy. When electrons are promoted in the conduction band with notable kinetic energy, their spin relaxation is first governed by the DP mechanism. Its efficiency strongly increases with kinetic energy and the depolarization is more pronounced for large $h\nu$. However, the detailed understanding of the PEDC's is intricate: Indeed, on the one hand, the polarization inside

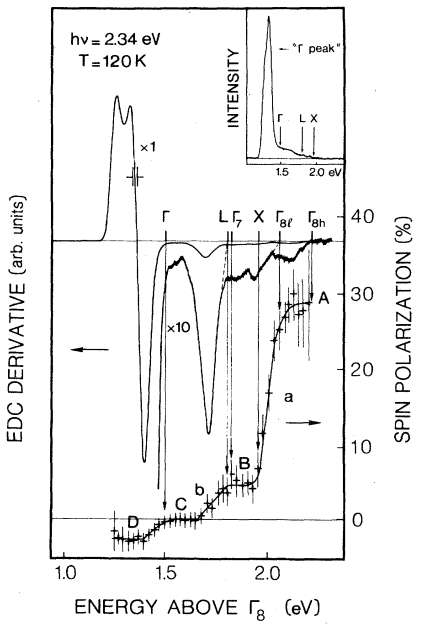

FIG. 3. EDC derivative and PEDC at 120 K of electrons emitted from NEA GaAs [(100), p-type $\sim 10^{19}$ cm^{-3}] for 2.34-eV excitation energy. Electron energy is referenced to the valence-band maximum Γ_8. The inset visualizes the shape of the EDC and emphasizes that the main contribution to the photoemitted current originates from the lower-energy peak, the so-called "Γ peak". The experimental resolution is represented by ⊣⊢ . The promotion energies of the electrons excited from the heavy-hole, light-hole, and spin-orbit-split valence bands are, respectively, labeled Γ_{8h}, Γ_{8l}, and Γ_7; the positions of the conduction-band extrema in the bulk are noted Γ, L, and X. These particular energies are determined by the extrapolation procedure described in I (Secs. IV A 1 and IV A 2) and shown by the dashed lines. They are marked with arrows on the PEDC. The bars on the PEDC indicate the statistical errors.

the solid is determined by the initial polarizations and the relative weights of the optical transitions, as well as by spin relaxation in the Γ or the side valleys. On the other hand, for a given electron kinetic energy, the photoemission polarization is not directly related to the polarization in the bulk crystal because the details of the escape process must be taken into account.

The photoemission polarization has been measured as a function of the electron kinetic energy for different exciting photon energies and at various temperatures. Figure 3 shows a low-temperature (120 K) PEDC for σ^- light excitation at $h\nu=2.34$ eV (unless otherwise specified, the results presented in the figures are obtained on sample 1). The EDC derivative is juxtaposed to relate the polarization structures to those identified in the EDC's and already interpreted in I. The following typical features are apparent.

(i) At the highest energy (PEDC portion marked A in Fig. 3), the electrons are promoted from the heavy-hole band and emitted without significant energy loss. The sharp decrease (a) originates from the onset of electrons excited from the light-hole band with a negative polarization [see Fig. 2(b)]. Spin relaxation during the first stages of energy loss also contributes to reduce the polarization.

(ii) The B plateau is due to electrons accumulated in the X minima of the crystal. Electrons created from the spin-orbit-split valence band are responsible for the decrease (b) of the polarization.

(iii) The following zero polarization plateau (C) results from the contribution of electrons thermalized in the L minima and undergoing efficient spin relaxation.

(iv) The last D plateau, corresponding to the dominant photoemission peak ("Γ peak"), reflects the polarization of the thermalized electrons in the bulk crystal. Before emission, these electrons have undergone energy and possibly spin relaxation in the band-bending region.

Figures 4 and 5 show PEDC's for several visible and near-infrared krypton-laser lines at 120 and 300 K. Note that two PEDC's measured on a $GaAs_{1-x}P_x$ sample are reproduced in Ref. 14; they do not show pronounced polarization variations since the excitation energy $h\nu \simeq 1.95$ eV is close to the band gap. They have to be compared to our 1.55-eV curves and indeed present the same behavior.

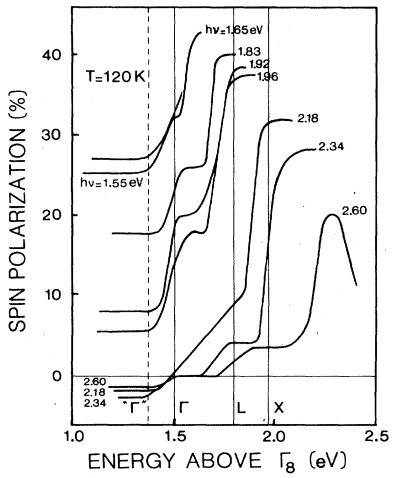

FIG. 4. PEDC's at 120 K for excitation by He-Ne and most of the Kr^+-laser lines. The bulk Γ, L, and X experimental positions are indicated by solid vertical lines; the dashed line shows the "Γ peak." The error bars (not indicated) are typically the same as those in Fig. 3; moreover, each curve was found to be very reproducible over a large number of experiments.

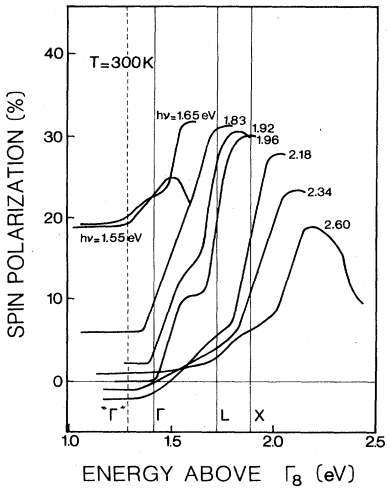

FIG. 5. PEDC's at 300 K for excitation by He-Ne and most of the Kr^+-laser lines. The locations of the bulk Γ, L, and X extrema, indicated by solid vertical lines, are calculated from our 120-K determinations using the temperature variation given in Ref. 25. The "Γ peak" position is marked by a dashed line.

We shall quantitatively analyze the high- and low-energy sides of the PEDC's, which present special features and are more suited for modelization. The discussion will mainly refer to the low-temperature data: In this case the situation is simpler because energy gain during a collision is much less probable than energy loss.

A. Highest energy electron polarization

At 120 K the most energetic electrons carry the largest polarization. They appear at the final energy of the $\Gamma_{8h} \rightarrow \Gamma_6$ transitions as seen on the EDC's (see Figs. 3 and 4; see also Sec. IV A 2 of I). Experimentally, the maximum polarization decreases from $\sim 45\%$ for near-band-gap excitation to $\sim 20\%$ for $h\nu=2.60$ eV. These results do not differ much for samples 1 and 2.

1. Spin precession at the highest promotion energy

We propose a model to interpret the polarization reduction at $\Gamma_{8h} \rightarrow \Gamma_6$ promotion energy. The details of the calculation are given in Appendix A and we present here a physical insight of the mechanism. Since our energy resolution ($\simeq 20$ meV) is smaller than the energy loss by emission of an optical phonon ($\simeq 30$ meV), we suppose that we select electrons excited from the heavy-hole band into an anisotropic distribution (see Sec. III A) and undergoing no collision before emission. This is strictly true at low temperature if the DPY momentum and energy-relaxation processes can be neglected.

The absorption coefficient α determines the electronic

distribution inside the crystal just after excitation; the mean free path l characterizes the probability of emission without suffering any collision. We note that in our photon energy range, the product αl remains small compared to unity. Indeed, when electrons cannot be scattered into the L valley, l is of the order of 0.1 μm and α^{-1} varies from 1 μm to 0.5 μm; when the L valley can be populated, l is approximately halved and α^{-1} decreases to 0.35 μm at 2.60 eV.[4] Qualitatively, the electrons are promoted within a distance $1/\alpha$ from the surface and those escaping without any collision originate from a typical radius l inside the crystal. During the transit time to the surface, of the order of l/v, where v is the electron velocity, each spin precesses around its DP field (see Sec. III C 1): When all electrons are considered, the resulting mean spin normal to the crystal surface is reduced in a way similar to that of the Hanle effect.[1] The surface transmission coefficient of a NEA photocathode does not vary much with the emission angle,[4] but cannot be accurately determined: The usual models assume the conservation of momentum parallel to the surface, a condition which is not fulfilled in the presence of a Cs layer.[40] We shall assume an isotropic transmission coefficient which does not appear in the calculation of the polarization. Under these hypotheses, the polarization $P_{\max}$ measured at $\Gamma_{8h}\rightarrow\Gamma_6$ promotion energy is given by (see Appendix A):

$$P_{\max}\simeq\frac{2}{3}\int_0^{2\pi}d\phi\frac{1}{2\pi}\int_0^{\pi/2}d\theta\frac{4\cos^3\theta\sin\theta}{1+|\vec{\omega}(\vec{k})|^2(l/v)^2}, \quad (7)$$

where θ is the angle between Oz and $\vec{k}$, ϕ is the azimuthal angle; the precession vector $\vec{\omega}(\vec{k})$ is defined in Sec. III C 1.

If spin precession is negligible, $P_{\max}$ is equal to $\frac{2}{3}$, in spite of a 100% polarization of the electrons excited from the heavy-hole band with momentum parallel to Oz [see Eq. (1)]. This results from angular averaging and could not be increased by angular selection in vacuum since momentum anisotropy is relaxed by the Cs layer.[40] Polarizations greater than 50% have indeed been reported by Pierce and Meier who measured 54%.[41] Yet, the largest polarization measured in our experiment does not exceed 50% ($\simeq$48% for sample 2 at $h\nu=1.65$ eV and 120 K).

In the same model and in the absence of depolarization in the DP field we have also calculated the photoemission polarization at promotion energy for electrons excited from the light-hole or spin-orbit-split bands. The results are plotted in Fig. 2(b) (dashed curves). Note that for near-band-gap excitation from the light-hole band, the angular integration yields a polarization of $\frac{2}{7}$, whereas the electrons with momentum parallel to Oz are -100% polarized.[29]

The $h\nu$ dependence of $P_{\max}$ is contained in the precession term $|\vec{\omega}(\vec{k})|^2(l/v)^2$. With the aid of formula (7), we estimate l from our measurements of $P_{\max}$ at 120 K. From the experimental near-band-gap value of $\omega^2(\epsilon)$,[35] we fit the constant B' in Eq. (4). Then, we take into account the energy variation of the other factors.[26] We find an almost constant mean free path $l\simeq0.12$ μm for $h\nu$ exceeding 1.96 eV, that is when the L valley can be populated. It increases to 0.25 μm when $h\nu$ decreases to 1.65 eV. These values correspond to a collision time l/v increasing from 5.10^{-14} s for electron kinetic energies $\sim$1 eV to 3.10^{-13} s for near-band-gap excitation, in good agreement with the estimations of Ref. 4 and the measurements reported in Refs. 42 and 43. Note that in I we showed that the EDC shape does not allow the determination of the mean free path in the way suggested by James and collaborators.[44,45] On the contrary, the present polarization analysis provides an estimation of this quantity as a function of the electron kinetic energy.

The present model explains satisfactorily the experimental $P_{\max}$ values except for very-near-band-gap excitation and also for $h\nu=2.60$ eV where the maximum polarization appears at an energy somewhat lower than the promotion energy. For $h\nu=1.55$ eV, the "Γ peak" and the hot-electron structure overlap, as seen on the EDC derivative presented in Fig. 7 of I, and this decreases $P_{\max}$. In the case of $h\nu=2.60$ eV, which is our largest photon energy, the warping of the heavy-hole band must be invoked: The more energetic electrons are excited along the $\langle 111\rangle$ direction with a relatively low polarization [50% along Oz, deduced from Eq. (1) with $\cos\theta=1/\sqrt{3}$].

In the neighborhood of the promotion energy, the polarization decrease (A and a regions in Fig. 3) is comparable to the one reported for hot luminescence,[46] which was explained by taking into account the DPY energy and momentum relaxation mechanisms.[30]

At room temperature, the situation becomes complicated by the fact that it is not strictly possible to select electrons emitted without suffering any collision: Indeed, in Fig. 5, a decreased polarization of the electrons at an energy exceeding the promotion energy is sometimes observed. Yet the same analysis of $P_{\max}$ can be performed on the 300-K data. Provided that the promotion energy and the DP frequency in formula (7) take into account the band-gap reduction with increasing temperature, the 300-K results are fairly well understood using the same collision times as at 120 K. Note that the increase in $P_{\max}$ when cooling the crystal is more pronounced for small photon energies [$P_{\max}(120\text{ K})/P_{\max}(300\text{ K})\simeq1.5$ for $h\nu=1.55$ eV, whereas it is $\simeq1$ for $h\nu=2.60$ eV; compare Figs. 4 and 5]. Our measurements are in contradiction with those of Allenspach *et al.*[47] who find a constant increase of the polarization at photoemission threshold. These authors compare the temperature variation of polarization at threshold for positive and negative electron affinities and observe that they are identical; they conclude in favor of the same surface depolarization mechanism, for all emitted electrons. Such an approach seems inadequate to us, since the fundamental differences between spin relaxation in the bulk crystal for hot electrons (DP mechanism; see above) and thermalized electrons (BAP mechanism; see Secs. III C 2 and IV C 2) are not taken into account.

2. *Hot-electron polarizations inside and outside the solid*

The whole depolarization at promotion energy is attributed here to the DP precession. Other mechanisms could be invoked for the polarization reduction: (i) We have neglected the admixture of remote bands in the wave functions, which may affect the polarization at large $h\nu$.

Their effect should be too small to be considered in our experiments; (ii) the electrons could also be depolarized when crossing the surface.

To discriminate between bulk and surface depolarization we have studied, in the same samples, the polarization of the hot photoluminescence which originates from hot-electron recombination on acceptor levels with heavy-hole symmetry.[11] Figure 6 shows the luminescence polarization as a function of the recombination photon energy, measured on sample 1 under 1.92-eV light excitation at 77 K. The curve presents two remarkable features: a sharp high-energy edge, corresponding to the polarization of the electrons excited from the heavy-hole band, and a dip to zero at the onset of the electrons excited from the light-hole band.[11] The maximum luminescence polarization we measure is 39%, which exceeds the 25% theoretical maximum value for an isotropic momentum distribution:[1] This is an experimental evidence of the anisotropy of the hot-electron distribution. Under the same conditions, for sample 2, we obtain 48% at $h\nu=1.92$ eV and 57% at $h\nu=1.65$ eV. These results agree with those of Ref. 11 where a 47% maximum polarization for $h\nu=1.96$ eV at 80 K is reported. However, the theoretical maximum luminescence polarization is $\frac{5}{7}$ (Ref. 29). The reduction of the hot-luminescence polarization is consistent with that of the maximum photoemission polarization and can also be understood from the DP mechanism.[11]

The present analysis confirms that the reduction of the hot photoemission polarization is a bulk rather than a surface effect,[48] a conclusion which will also be supported by the study of the low-energy part of the PEDC's (see Sec. IV C 3).

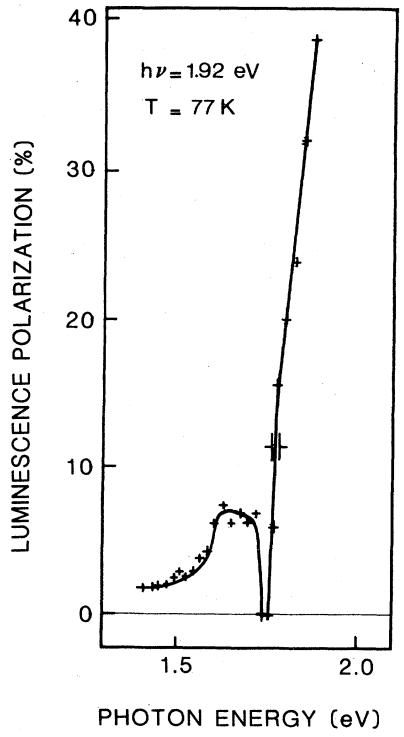

FIG. 6. Polarization of hot photoluminescence at 77 K under 1.92-eV excitation.

B. Intermediate energies

Between the maximum excitation energy and the bottom of the conduction band in the bulk crystal, the PEDC's generally show up a succession of plateaus. At a given kinetic energy, the overall polarization results from the contributions of electrons promoted from several valence bands and having suffered different relaxation processes. A quantitative analysis would be very intricate and here we qualitatively comment on the essential features of the PEDC's in that region by reference to the EDC studies of I (Sec. IV A 2). We also derive some information on the energy-relaxation channels. The discussion refers to the 120-K data (Fig. 4), similar conclusions also apply to the room-temperature results.

At an energy somewhat lower than the final state of the $\Gamma_{8h}\rightarrow\Gamma_6$ transition, the polarization shows a steep decrease versus energy. For near-band-gap excitation ($h\nu<1.83$ eV) the corresponding polarization reduction is not very pronounced and is a consequence of the "mixing" between the thermalized and the hot electrons. At $h\nu\geq 1.83$ eV, the polarization is partly reduced by DP relaxation but it essentially drops at the onset of the electrons promoted from the Γ_{8l} band with reduced or negative polarization.

For 1.65 eV $\leq h\nu<2.34$ eV, a small plateau or a slope occurs for electrons appearing between the Γ and L bulk positions. The origin of this structure is complicated as it arises from various contributions: high-energy tail of the thermalized distribution in Γ, nonthermalized electrons promoted from the Γ_{8h},Γ_{8l}, and (for $h\nu\geq 1.92$ eV) Γ_7 bands, or accumulated in the L minima (when energetically possible).

For $h\nu\geq 2.34$ eV, two higher-energy plateaus are observed: They correspond to the emission of electrons accumulated in the L and X valleys (C and B plateaus in Fig. 3). In these side minima, the spin splitting of the conduction band differs from that of the Γ valley.[49] It should produce a spin-relaxation mechanism, analogous to the DP process, the efficiency of which is difficult to estimate. In this photon energy range, we observe a zero polarization plateau mainly corresponding to electrons excited from the two upper valence bands, which have reached the L minima and there suffered efficient spin relaxation. We have seen (Sec. IV B 3 of I) that these electrons appear at an energy lower than that of the bulk L position. Before emission, they have lost their energy either in the bulk Γ valley or in the L band-bending region. We now prove by contradiction that the latter situation occurs: We assume that this plateau, which ends at the bulk Γ minimum, originates from electrons backscattered into the Γ valley prior to emission. As their momenta are isotropic because of multiple phonon collisions, the photoemission polarization reflects the angle averaged Γ valley polarization so that the "Γ peak" will also be unpolarized, which is not the case. We conclude that the L electrons relax their energy in the L band-bending region before being emitted and also that the negative polarization of the Γ electrons is mostly due to the contribution of the elec-

trons excited from the spin-orbit-split band which have reached the Γ point without energy or spin relaxation in the side valleys. The occurrence of an X plateau also suggests that the X electrons relax their energy in the band-bending region and that the DP process in the X valley is less efficient than in Γ. Indeed, if these electrons were backscattered into Γ, they would get a sufficiently high kinetic energy ($\simeq$460 meV) to be depolarized. Note that, on both 2.34- and 2.60-eV curves, the low-energy edge of the X plateau coincides with the promotion energy from the spin-orbit-split band.

C. Lower energies

The main contribution to the current emitted by a NEA photocathode arises from the "Γ-peak" region, located below the bulk Γ energy in the solid (portion D of the PEDC's in Fig. 3; see also Sec. IV B 1 of I). Its polarization P_e determines the overall polarization of the electron beam in vacuum when no energy selection is performed, and results from the cumulated effects of the spin-relaxation processes described in Secs. III B and III C.

1. Results

For near-band-gap excitation, a high spin polarization is observed (20—30 %; see Figs. 4 and 5) as the electrons are excited close to the Γ minimum from the Γ_{8h} and Γ_{8l} bands only, with a 50% angular averaged polarization. They are only depolarized in the thermalized state. Notice that in Figs. 4 and 5, P_e (1.65 eV) is greater than P_e (1.55 eV); for sample 2, the reverse occurs and the origin of this discrepancy is unclear.

For higher excitation energies, the depolarization during the thermalization step must also be considered. Indeed at $T=120$ K and $h\nu=1.83$ eV, an energy which does not allow $\Gamma_7\rightarrow\Gamma_6$ transition, P_e is approximately halved, and the reduction of the $\Gamma_{8l}\rightarrow\Gamma_6$ mean polarization to ~25% [see Fig. 2(b)] is insufficient to explain this result. We attribute the decrease of P_e to the DP process which becomes the dominant spin-relaxation mechanism in this energy range.[12]

For $h\nu=1.92$ eV, a photon energy which allows electron excitation from the three valence bands, P_e is smaller, and positive. It is almost zero for $h\nu=1.96$ eV, and becomes negative (~ −1 to −2 %) for higher photon energies. In these cases, the light-hole band is deeply modified, resulting in a negative contribution. Moreover, the $\Gamma_7\rightarrow\Gamma_6$ transition also promotes electrons of negative polarization. As the electrons excited from the Γ_{8h} band have the largest kinetic energy, they suffer the strongest DP spin relaxation so that the overall polarization P_0 of the electrons reaching Γ [see Eq. (2)] is negative. A sign reversal of the thermalized polarization was also reported in luminescence experiments performed on slightly less doped samples.[50,51] Thus, for large photon energies, we generally obtain a negative thermalized photoemission polarization; an exception is the slightly positive P_e obtained at 300 K for $h\nu=2.60$ eV. This particularity can be understood in the following way: For this photon energy, the final states of the three Γ_{8h}, Γ_{8l}, $\Gamma_7\rightarrow\Gamma_6$ transitions lie well above the energy of the L minima, so that all photoelectrons are relaxed in a similar way through these side valleys. In particular, most of the negatively polarized electrons excited from the Γ_7 band have been depolarized in the L valleys so that the overall polarization P_e is dominated by the small residual positive contribution of electrons excited from the two upper valence bands.

2. Comparison between polarizations in the solid and in vacuum

To quantitatively interpret our photoemission results, we analyze them in relation with luminescence data (see Sec. III D 2) and use the diffusion model quoted in (i) of Sec. III D 1. The thermalized polarization $P_{\text{therm}}(h\nu)$ is measured using the photoluminescence technique and we deduce τ/T_1 ratios. We find for sample 1 (sample 2) $\tau/T_1\sim1.1$ (0.25) at 120 K and 5.6 (0.9) at 300 K. Assuming that the lifetime τ does not appreciably vary with temperature T,[12,52] the decrease of τ/T_1 when cooling the crystal is in qualitative agreement with the $T^{-3/2}$ dependence of the BAP mechanism in our temperature range.[13] To conveniently compare the polarizations inside and outside the solid, we note that for near-band-gap excitation:

$$P_{\text{therm}}(h\nu)=P_{\text{therm}}(E_G)=0.5T_1/(T_1+\tau)$$

and rewrite Eq. (5) as

$$P_e(h\nu)=P_{\text{therm}}(h\nu)[2P_{\text{therm}}(E_G)]^{-1/2}. \quad (8)$$

We have plotted in Fig. 7 the measured $P_e(h\nu)$ as a function of the values deduced from Eq. (8) for samples 1 and 2. The results of Ref. 37 are also plotted as "sample 3." We indeed observe that both quantities are proportional but that the measurement generally provides a lower value. In samples 1 and 2, for $h\nu$ close to E_G, P_e increases with decreasing temperature by a factor of 1.4 (sample 1) or 1.3 (sample 2), in agreement with the data of Refs. 47 and 53—55.

The discrepancies observed in Fig. 7 between the predicted P_e value and the measurement evidence that an

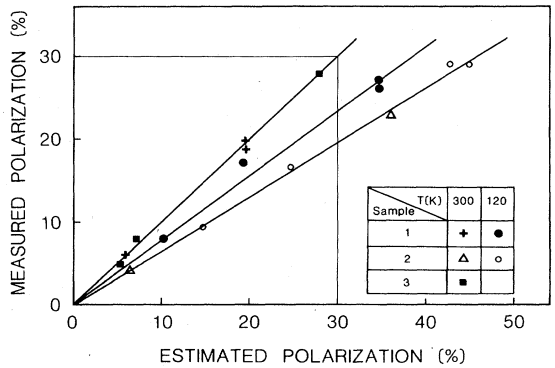

FIG. 7. Comparison between the measured polarization of the electrons emitted at an energy lower than the bulk Γ position and the value calculated from Eq. (8). At 300 K for $h\nu=1.55$ eV, the thermalized electron polarization, $P_{\text{therm}}(E_G)$, deduced from luminescence is 8% for sample 1 and 26% for sample 2; at 120 K, it increases to 24% for sample 1 and 40% for sample 2. For "sample 3" at 300 K, $P_{\text{therm}}(E_G)=16\%$ (results taken from Ref. 37).

additional sample and temperature-dependent depolarization occurs in the photoemission process. In Refs. 53 and 54, a depolarization during the emission into vacuum was also invoked but the expected values of P_e were deduced from luminescence data taken in the literature. As the ratio $T_1/(T_1+\tau)$ is sample dependent, it is impossible to discriminate between bulk and surface relaxations. In these papers, such an effect was attributed to exchange scattering in the Cs-O-Cs overlayer. As the experimental polarizations do not depend on the conditions of activation, we exclude this hypothesis, in agreement with Ref. 47.

3. *Additional spin relaxation in the escape process*

Additional depolarization of thermalized and hot electrons could arise from the same relaxation mechanism at the surface, as proposed in Ref. 47, such as, for instance, interaction with paramagnetic defects. Yet our measurements indicate that the two phenomena are of different nature: indeed for sample 1 at 300 K, the measured P_e values follow exactly Eq. (8), i.e., no additional depolarization occurs during the escape process, but the $P_{\max}$ values are slightly smaller than in the case of sample 2, for which a notable reduction of P_e is observed.

We propose a depolarization model involving spin relaxation in the band-bending region, where most electrons are trapped prior to emission. In this region, the electrons get a kinetic energy ϵ' of the order of the band bending δV ($\delta V \sim 0.5$ eV; see Sec. IV B 1 of I) relative to the bottom of the conduction band near the surface. They lose their spin orientation through the DP mechanism, efficient at such kinetic energies, while relaxing their energy.[56] The calculation is given in Appendix B: for reasonable characteristic times, the polarization at the bottom of the conduction band near the surface may be reduced by a factor ~ 1.4 through this process, the whole depolarization taking place in the first 200-meV energy loss. Obviously, the reduction factor does not depend on $h\nu$. These results fit qualitatively well with the experiment as we observe a depolarization in the first 130 meV of the band bending and then a polarization plateau. In fact, a spin-relaxation mechanism other than the DP process could also account for our experimental data provided it is energy dependent and efficient only for energies exceeding a few tenths of an eV. A modification of the spin relaxation close to the surface was also suggested to interpret polarized luminescence data.[57,58] Nevertheless, the BAP mechanism, which was invoked for spin relaxation in the band-bending region of $GaAs_{1-x}P_x$ in Ref. 14, must be discarded as its efficiency is strongly reduced because of hole depletion.

To summarize, the one-dimensional diffusion model cannot alone account for the photoemission polarization of thermalized electrons for all samples and temperatures, but it thoroughly describes the depolarization in the bulk crystal; the inclusion of additional spin relaxation near the surface allows a complete interpretation of the experimental data.

V. GaAs PHOTOCATHODES: IMPROVED ELECTRON SOURCES

Intense monochromatic and/or polarized electron sources are of great interest in many fields of experimental physics. For some years, GaAs photocathodes have proved to be very convenient polarized electron sources. In a previous paper,[9] we reported for the first time that GaAs photocathodes are also, under proper preparation conditions, very intense monokinetic electron sources: an improvement in intensity up to 3 orders of magnitude over standard monochromatized electron guns may be reasonably expected. A collision physics experiment using a GaAs monoenergetic electron source is now at work.[59] We give here some additional information on the operation and performances of such a polarized and monokinetic electron source, using the concepts exposed in the preceding sections of this paper as well as in I.

A. Polarized electron sources

Under circularly polarized light excitation of energy close to the band gap, the mean polarization of the photoemitted beam usually ranges from 20% to 30% at 300 K and reaches 25–45% at low temperature[5,6,47,53–55,60–65] (we except here the very particular case of the samples grown by molecular-beam epitaxy for which higher polarizations are reported[66,67]). We have indeed measured that the polarization of the electrons which, in the bulk crystal, were thermalized at Γ is $\sim 20\%$ at 300 K and reaches $\sim 30\%$ at 120 K. However, the comparison between these results and the values quoted in the literature is intricate for several reasons: (i) the bulk characteristic times τ and T_1 strongly vary with the samples, even for comparable doping levels; (ii) the influence of the emitting face orientation, which is not completely clarified,[56,61] is still complicated by possible faceting; (iii) the vacuum level location is not usually specified whereas the spin polarization depends on the electron kinetic energy; (iv) the *absolute* value of the polarization is not accurately known (see Sec. II).

The increase of polarization when cooling the crystal arises from the increase of the spin relaxation time T_1 associated with the BAP mechanism (see Sec. IV C 2). However, an additional depolarization, which depends on both temperature and sample, occurs during the emission. Then, the temperature variation of the photoemission polarization cannot be exactly predicted.

It was shown[53,54] that running the source with a positive affinity permits to achieve high polarization for notable $h\nu$ (1.96 eV, for instance). Indeed, it is now well established that the polarization generally rises with the aging of the photocathode.[53,54,65,68] This behavior is clearly understood from our PEDC's: when the vacuum level is sufficiently high only the electrons promoted from the heavy-hole band, which are highly polarized, can escape from the solid. We can also understand why no polarization increase with aging of the cathode or with electron kinetic energy was observed for $h\nu = 1.53$ eV in Refs. 6 and 69: In this special case, the photon energy is so close

to E_G that the hot-electron structures must disappear in the thermalized peak, leading to a constant polarization as a function of the electron kinetic energy (our 1.55-eV curves in Figs. 4 and 5 show an attenuated polarization variation).

B. Monokinetic electron sources

The high-energy tail of the EDC's is due either to electrons accumulated in the side valleys of the crystal or to hot electrons. It approximately ends at the maximum promotion energy, from the heavy-hole band, and for near-band-gap excitation its extent becomes negligible. As the affinity acts as a high-pass-energy filter and truncates the low-energy part of the photoemitted electron distribution, we may, at a given photon energy, adjust the FWHM of the EDC by controlling the vacuum level position. After optimum activation, it is easy to raise the work function of the surface, for instance, by adding small oxygen amounts (see Fig. 8). An alternative procedure consists in waiting for the aging of the photocathode: This leads in the same way to a narrowed electron distribution (see Fig. 13 of I). Moreover, the FWHM of the distribution and the emitted intensity can be independently adjusted: We verified over a wide range of light intensities that the total emitted current is proportional to the number of absorbed photons, with no modification of the EDC shape (Fig. 9). Figure 10 shows, at room temperature and for $h\nu = 1.55$ eV, a 100-meV FWHM EDC with 2.5% quantum yield. Such a performance, which improves by 1 order of magnitude the values quoted in the literature,[69] il-

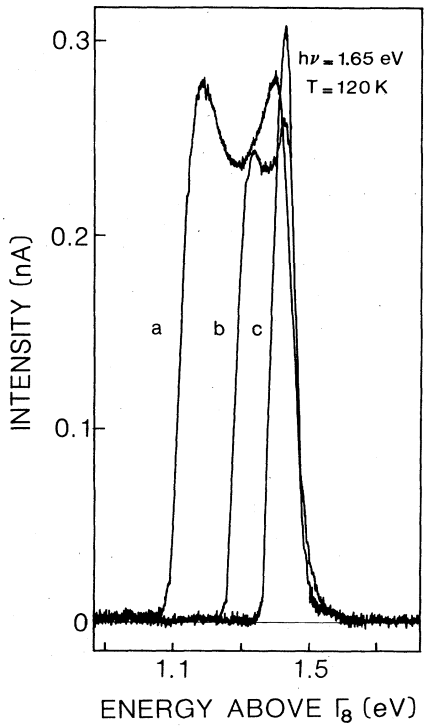

FIG. 8. EDC at 120 K for 1.65-eV photon energy. The ordinate is the selector output current. The effective electron affinity is very low in the case of curve *a* (−0.45 eV). The photocathode is then exposed to a weak oxygen pressure ($\sim 1.10^{-10}$ Torr) during a few minutes which increases the electron affinity (curves *b* and *c*). By such a procedure we adjust the vacuum level location in order to achieve a 60-meV FWHM distribution (curve *c*).

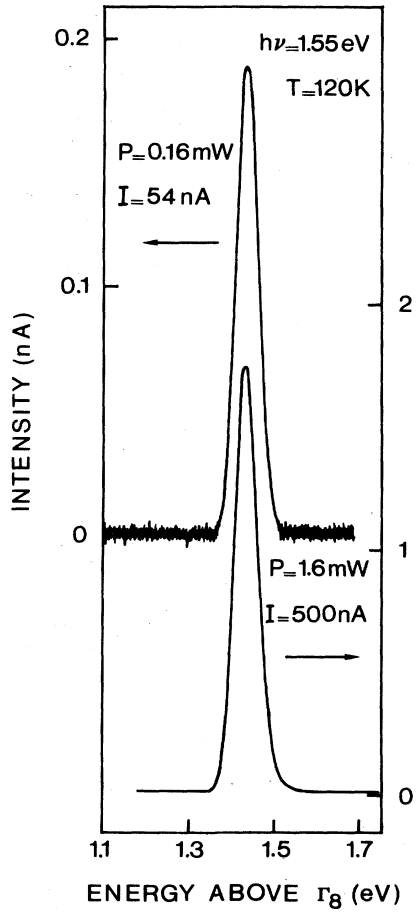

FIG. 9. EDC's at 120 K for 1.55-eV excitation energy. The proportionality between the photoemitted current and the light power is evidenced in these experimental conditions.

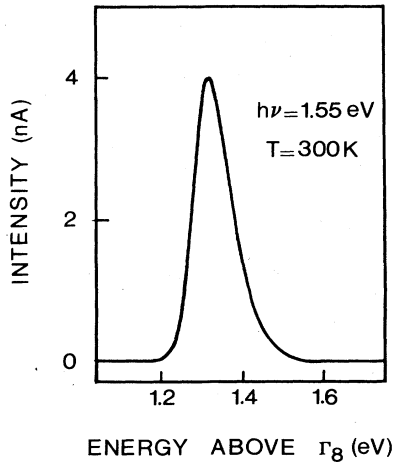

FIG. 10. EDC at 300 K, measured on sample 2 for 1.55-eV excitation energy. The FWHM of this distribution is 100 meV and the quantum yield as high as 2.5%.

lustrates the possibilities of GaAs as an intense monokinetic electron source. If distributions narrower than ~ 100 meV are required, the photocathode must be cooled and operated with a slightly negative electron affinity: We indeed find (see Sec. IV B 2 of I) that, in these conditions, the high-energy tail of the "Γ peak" is nearly Maxwellian, with an effective temperature decreasing with lattice temperature. We are then able to obtain distributions as narrow as 30 meV (see Fig. 12 of I). Similar performances are also obtained using the 1.65-eV Kr^+-laser line: The only difference is the presence of a small hot-electron structure at the high-energy end of the EDC (see Fig. 7 of I). Note that these conditions, which provide monokinetic electrons, also lead to highly polarized beams.

C. Stability

Very clean preparation conditions are necessary to achieve stable sources. We found that the best way is to activate the sample at a pressure as low as possible (in the low 10^{-10}-Torr range). It is probably because of these special precautions that we observe an increase of the quantum yield when cooling the crystal, at the difference of Ref. 6 where adsorption of residual cesium was assumed to reduce the yield at low temperature. With respect to time, the photocurrent decreases ($\sim 1\%$ per h) as a consequence of the rise of the electron affinity (see Sec. IV B 1 of I). After low-temperature operation, warming up the sample permits to desorb cryopumped gases and restores most of the initial yield. At room temperature the photocathode can be rejuvenated by deposing cesium. Neither these procedures nor complete reactivation including thermal treatment deteriorate the source characteristics.

VI. CONCLUSION

This detailed study of the spin polarization versus kinetic energy of the electrons emitted from an optically-pumped GaAs photocathode evidences peculiarities of the semiconductor band structure and spin-relaxation effects in the bulk crystal as well as in the band-bending region. From the PEDC's, it is clear that the spin relaxation of conduction electrons at kinetic energies exceeding a few tenths of an eV plays a determinant part in the polarization of the photoemitted electrons, in complete agreement with theoretical predictions. Typical polarization structures are observed and related to those occurring in the EDC's, already interpreted in I. In two cases a quantitative evaluation of the photoemission polarization is carried out.

(i) For the electrons emitted at the highest promotion energy, where the spin polarization is reduced by spin precession in the internal magnetic field during the transit time to the surface. An estimate of the hot-electron mean free path is deduced from the polarization measurements, in fair agreement with previous data. Such an estimate cannot be obtained from the only EDC results (see Sec. IV C 4 of I).

(ii) For the electrons which were first thermalized at the bulk Γ minimum. A comparison of their polarization with that of the electrons thermalized at Γ in the solid, measured through luminescence, evidences an additional depolarization in the emission process. It may be understood in terms of spin relaxation in the band-bending region. The PEDC's also allow to discriminate between several energy-relaxation channels for the electrons which were accumulated at the bottom of the side valleys.

Our experiments have shown that greatly improved monochromatic electron sources are now achievable, offering new possibilities to collision physics: An electron distribution of a few percent quantum yield with an energy width of ~ 100 meV is obtained at 300 K; at 120 K it is possible to narrow the distribution to 30 meV at the expense of the yield (a few hundredths of a percent; we recall that for near-band-gap excitation a 1% yield corresponds to ~ 6-μA/mW light excitation). Up to now, no attempt has been made to optimize the performances of these monoenergetic electron sources, in particular, by lowering the temperature. The present results have confirmed the usual values of the spin polarization obtained for negative-electron-affinity GaAs photocathodes under near-band-gap circularly polarized excitation ($\sim 20\%$ at 300 K, $\sim 30\%$ at 120 K). Using the fundamental properties of the photoemission of GaAs studied in this paper and in I, we have given a physical understanding of the operation and performances of monoenergetic and polarized GaAs electron sources.

ACKNOWLEDGMENTS

We gratefully acknowledge the participation of M. Eminyan at the initiation and during the early stages of this experiment. We are indebted to D. M. Campbell for the supply of the Mott polarimeter and for useful advice, and D. Paget for pertinent remarks on the manuscript. We have benefited from helpful discussions with J.-N. Chazalviel, G. Fishman, J.-F. Gouyet, J.-P. Hermann, R. Houdré, P. Jarry, D. Paget, C. Piaget, and A. Tardella. We thank C. Vasseur for technical help. One of us (H.-J.D.) wishes to express his thanks to the Mission Recherche de la Délégation Générale pour l'Armement and to the Direction des Recherches, Etudes et Techniques which made it possible for him to accomplish this work. Laboratoire de Physique de la Matière Condensée is Groupe de Recherche 050038 du Centre National de la Recherche Scientifique.

APPENDIX A

We calculate the polarization of electrons emitted at their promotion energy without suffering any collision. The probability of electron promotion at a distance z within dz normal to the surface by absorption of a photon of energy $h\nu$ is equal to

$$dn(z)=\alpha \exp(-\alpha z)dz \ , \tag{A1}$$

where α is the light absorption coefficient at this photon energy. Such an electron has a probability $\exp(-z/l|\cos\theta|)$ to reach the surface without suffering any collision; $\theta \in [\pi/2;\pi]$ is the angle between the incident- light direction Oz and the momentum $\vec{k}$ (of modulus k); l is the electron mean free path. For a velo-

city v, the transit time to the surface is $t=z/v\,|\cos\theta|$.

We consider the electrons promoted by the $\Gamma_{8h}\rightarrow\Gamma_6$ transition. For σ^- excitation, their spin $\vec{S}(\vec{k})$ is given by[27,29]

$$\vec{S}(\vec{k})=\frac{\cos\theta}{1+\cos^2\theta}\frac{\vec{k}}{k} \tag{A2}$$

and their number $n(\theta)$ is equal to $1+\cos^2\theta$ with suitable normalization. In our experiment, we measure the total spin component along Oz. During t, each spin experiences the DP field $\vec{\omega}(\vec{k})$ so that its component $S_z(\vec{k},t)$ along Oz is modified according to

$$\frac{S_z(\vec{k},t)}{\vec{S}(\vec{k})\cdot\vec{k}/k}=\cos[\,|\,\vec{\omega}(\vec{k})\,|\,t]\frac{\vec{k}\cdot\vec{z}}{k} -\sin[\,|\,\vec{\omega}(\vec{k})\,|\,t]\frac{(\vec{\omega}(\vec{k}),\vec{k},\vec{z})}{|\,\vec{\omega}(\vec{k})\,|\,k}\,, \tag{A3}$$

where $\vec{z}$ is the unit vector along Oz. The DP field is characterized by the precession vector $\vec{\omega}(\vec{k})$ defined in Sec. III C 1.

The total number of electrons reaching the surface is

$$\bar{n}=\frac{1}{4\pi}\int_0^\infty dz\int_{\pi/2}^{\pi}d\theta\int_0^{2\pi}d\phi\,\alpha\exp\left[-z\left[\alpha+\frac{1}{l\,|\cos\theta|}\right]\right]n(\theta)\sin\theta\,, \tag{A4}$$

where ϕ is the azimuthal angle. The total spin momentum along Oz is equal to

$$\bar{M}_z=\frac{1}{4\pi}\int_0^\infty dz\int_{\pi/2}^{\pi}d\theta\int_0^{2\pi}d\phi\,\alpha\exp\left[-z\left[\alpha+\frac{1}{l\,|\cos\theta|}\right]\right]n(\theta)S_z(\vec{k},t)\sin\theta\,. \tag{A5}$$

In our physical conditions $\alpha l\ll 1$, so that we evaluate (A4) and (A5) to first order in αl. We find

$$\bar{n}=\tfrac{3}{8}\alpha l\,. \tag{A6}$$

Only the first term in (A3) contributes to $\bar{M}_z$, which can be written as

$$\bar{M}_z=\frac{1}{4\pi}\int_0^{2\pi}d\phi\int_0^{\pi/2}d\theta\frac{\alpha l\cos^3\theta\sin\theta}{1+|\,\vec{\omega}(\vec{k})\,|^2(l/v)^2}\,. \tag{A7}$$

We deduce $P_{\max}=2\bar{M}_z/\bar{n}$:

$$P_{\max}=\frac{2}{3}\int_0^{2\pi}d\phi\frac{1}{2\pi}\int_0^{\pi/2}d\theta\frac{4\cos^3\theta\sin\theta}{1+|\,\vec{\omega}(\vec{k})\,|^2(l/v)^2}\,. \tag{A8}$$

The squared precession vector $|\,\vec{\omega}(\vec{k})\,|^2$ is related to its angular average $\omega^2(\epsilon)$ by

$$|\,\vec{\omega}(\vec{k})\,|^2=\tfrac{35}{4}\omega^2(\epsilon)(1-\cos^2\theta)[\cos^2\theta+\tfrac{1}{4}\sin^2 2\phi\sin^2\theta(1-9\cos^2\theta)]\,, \tag{A9}$$

since for our crystal orientation Oz is along $\langle 100\rangle$.[12,32]

The expression (4) of $\vec{\omega}(\vec{k})$ involves a and b Kane coefficients for the conduction band.[26] Only for a small kinetic energy ϵ, when the conduction band is parabolic, do these coefficients have the values given in Ref. 12:

$$a=1-\gamma(\epsilon/E_G)\,,$$

$$b=\beta(\epsilon/E_G)^{1/2}\,,$$

where γ and β are constants related to band parameters. In these conditions $\omega^2(\epsilon)$ increases nearly as $(\epsilon/E_G)^3$ and the reduction of E_G with increasing temperature produces an increase in $\omega^2(\epsilon)$. For larger kinetic energies, the product ab decreases and becomes zero when the conduction band remains coupled to the sole spin-orbit-split band.[26] We numerically evaluate Eq. (A8) from the Kane model in order to determine l. For simplicity, ϵ and v are taken in the parabolic approximation. The application of formula (A8) to our experimental data is given in the main text (see Sec. IV A 1).

APPENDIX B

We calculate the polarization of the electrons which were thermalized at the bottom of the conduction band in the solid and are emitted after energy relaxation in the band-bending region. Consider the plane parallel to the crystal face which limits the band-bending region inside the crystal. The recombination velocity at this plane is comparable to the usual surface recombination velocity. Then, in the diffusion model, the polarization $P_s(h\nu)$ of the electrons penetrating into the band-bending region is deduced from Eq. (5):

$$P_s(h\nu)=P_{\text{therm}}(h\nu)[T_1/(T_1+\tau)]^{-1/2}\,. \tag{B1}$$

Most electrons are trapped in the band bending prior to emission. They get a kinetic energy $\epsilon'\sim\delta V$ relative to the bottom of the conduction band near the surface (the band bending δV is ~ 0.5 eV) and lose spin orientation through the DP mechanism during their energy relaxation. Because of hole depletion, the only efficient energy-

relaxation process is collision with optical phonons. The corresponding characteristic time τ_{po} and the mean energy loss both depend on temperature approximately through the factor[70] $1/(2N_q+1)$, where the number of optical phonons N_q at a given temperature is given by the Planck formula. Consequently the kinetic energy ϵ' decreases with time t almost independently of temperature, according to the relation

$$\epsilon' = \delta V - \hbar\omega_o t/\tau_{po}^0 , \tag{B2}$$

where τ_{po}^0 refers to the low-temperature value of τ_{po}. The momentum relaxation time τ_p in the band bending is greatly shortened,[71] in particular, because of multiple reflections at the surface (the typical flight time l_D/v is $\sim 10^{-14}$ s, where $l_D \sim 100$ Å is the band-bending width), so that we assume $\tau_p \ll \tau_{po}$. In these conditions, the polarization $P_b(\epsilon')$ in the band-bending region can be calculated from the following equation:[12]

$$dP_b(\epsilon')/dt = -P_b(\epsilon')/\tau_s(\epsilon') . \tag{B3}$$

In the energy range such that $\omega^2(\epsilon)$ is proportional to ϵ^3, a straightforward integration yields:

$$P_b(\epsilon') = P_s \exp\{-\omega^2(\epsilon')\tau_{po}^0\tau_c[(\delta V/\epsilon')^4 - 1]\epsilon'/6\hbar\omega_o\} , \tag{B4}$$

where τ_c is the correlation time defined in Sec. III C 1, of the order of τ_p. Using $\tau_c = 10^{-14}$ s and $\tau_{po}^0 = 10^{-13}$ s, we find that the polarization at the bottom of the conduction band near the surface is reduced by a factor of ~ 1.4. The whole depolarization, which does not depend on $h\nu$, takes place in the first 200-meV energy loss.

[1] G. Lampel, in *Proceedings of the 12th International Conference on the Physics of Semiconductors, Stuttgart, 1974,* edited by M. H. Pilkuhn (Teubner, Stuttgart, 1974), p. 743, and references therein.

[2] *Optical Orientation,* Vol. 8 of *Modern Problems in Solid State Sciences,* edited by F. Meier and B. P. Zakharchenya (Elsevier, Amsterdam, 1984).

[3] J. J. Scheer and J. Van Laar, Solid State Commun. **3**, 189 (1965).

[4] C. Piaget, Thèse de Doctorat d'Etat, Université de Paris—Sud, Centre d'Orsay, 1977, and references therein.

[5] D. T. Pierce, F. Meier, and P. Zürcher, Appl. Phys. Lett. **26**, 670 (1975).

[6] D. T. Pierce, R. J. Celotta, G.-C. Wang, W. N. Unertl, A. Galejs, C. E. Kuyatt, and S. R. Mielczarek, Rev. Sci. Instrum. **51**, 478 (1980).

[7] H.-J. Drouhin, C. Hermann, and G. Lampel, preceding paper [Phys. Rev. B **31**, 3859 (1985)].

[8] A. L. Musatov, V. L. Korotkikh, and V. D. Shadrin, Fiz. Tverd. Tela (Leningrad) **23**, 929 (1981) [Sov. Phys.—Solid State **23**, 540 (1981)].

[9] H.-J. Drouhin, C. Hermann, M. Eminyan, and G. Lampel, J. Phys. (Paris) Lett. **44**, L1027 (1983).

[10] H.-J. Drouhin, C. Hermann, M. Eminyan, and G. Lampel, in *Proceedings of the 17th International Conference on the Physics of Semiconductors, San Francisco, 1984,* edited by D. J. Chadi (Springer, New York, in press).

[11] B. P. Zakharchenya, D. N. Mirlin, V. I. Perel', and I. I. Reshina, Usp. Fiz. Nauk. **136**, 459 (1982) [Sov. Phys.—Usp. **25**, 143 (1982)], and references therein.

[12] G. Fishman and G. Lampel, Phys. Rev. B **16**, 820 (1977).

[13] A. G. Aronov, G. E. Pikus, and A. N. Titkov, Zh. Eksp. Teor. Fiz. **84**, 1170 (1983) [Sov. Phys.—JETP **57**, 680 (1983)].

[14] J. Kirschner, H. P. Oepen, and H. Ibach, Appl. Phys. A **30**, 177 (1983).

[15] D. M. Campbell, C. Hermann, G. Lampel, and R. Owen, in Proceedings of the International Symposium on Polarization and Correlation in Electron-Atom Collisions, Münster, Federal Republic of Germany, 1983 (unpublished); D. M. Campbell, C. Hermann, G. Lampel, and R. Owen (unpublished).

[16] J. Van Klinken, Nucl. Phys. **75**, 161 (1966), and references therein.

[17] M. S. Lubell, G. D. Fletcher, and T. J. Gay, in Proceedings of the International Symposium on Polarization and Correlation in Electron-Atom Collisions, Münster, Federal Republic of Germany, 1983 (unpublished).

[18] M. Kaliswaart, M. R. O'Neill, T. W. Riddle, F. B. Dunning, and G. K. Walters, Phys. Rev. B **17**, 1570 (1978).

[19] J. Kirschner and R. Feder, Phys. Rev. Lett. **42**, 1008 (1979).

[20] M. Erbudak and N. Müller, Appl. Phys. Lett. **38**, 575 (1981).

[21] H. C. Siegmann, D. T. Pierce, and R. J. Celotta, Phys. Rev. Lett. **46**, 452 (1981).

[22] M. Erbudak and G. Ravano, J. Appl. Phys. **52**, 5032 (1981).

[23] D. T. Pierce, S. M. Girvin, J. Unguris, and R. J. Celotta, Rev. Sci. Instrum. **52**, 1437 (1981).

[24] G. F. Koster, J. O. Dimmock, R. G. Wheeler, and H. Statz, *Properties of the Thirty-Two Point Groups* (MIT, Cambridge, Mass., 1963).

[25] J. S. Blakemore, J. Appl. Phys. **53**, R123 (1982), and references therein.

[26] E. O. Kane, J. Phys. Chem. Solids **1**, 249 (1957).

[27] H.-J. Drouhin, Thèse de Doctorat d'Etat, Université de Paris—Sud, Centre d'Orsay, 1984.

[28] V. D. Dymnikov, I. I. Reshina, and V. F. Sapega, Fiz. Tverd. Tela (Leningrad) **23**, 731 (1981) [Sov. Phys.—Solid State **23**, 415 (1981)].

[29] V. D. Dymnikov, M. I. D'yakonov, and V. I. Perel', Zh. Eksp. Teor. Fiz. **71**, 2373 (1976) [Sov. Phys.—JETP **44**, 1252 (1976)].

[30] M. I. D'yakonov, V. I. Perel', and I. N. Yassievich, Fiz. Tekh. Poluprovodn. **11**, 1364 (1977) [Sov. Phys.—Semicond. **11**, 801 (1977)].

[31] D. G. Seiler, W. M. Becker, and L. M. Roth, Phys. Rev. B **1**, 764 (1970).

[32] M. I. D'yakonov and V. I. Perel', Zh. Eksp. Teor. Fiz. **60**, 1954 (1971) [Sov. Phys.—JETP **33**, 1053 (1971)].

[33] M. I. D'yakonov and V. I. Perel', Fiz. Tverd. Tela (Leningrad) **13**, 3581 (1971) [Sov. Phys.—Solid State **13**, 302 (1972)].

[34] A. Abragam, *The Principles of Nuclear Magnetism* (Clarendon, Oxford, 1961).

[35] V. I. Safarov and A. N. Titkov, in Proceedings of the 15th International Conference on the Physics of Semiconductors, Kyoto, 1980 [J. Phys. Soc. Jpn. Suppl. A **49**, 623 (1980)].

[36] G. L. Bir, A. G. Aronov, and G. E. Pikus, Zh. Eksp. Teor. Fiz. **69**, 1382 (1975) [Sov. Phys.—JETP **42**, 705 (1976)].

[37]G. Lampel and M. Eminyan, in Proceedings of the 15th International Conference on the Physics of Semiconductors, Kyoto, 1980 [J. Phys. Soc. Jpn. Suppl. A **49**, 627 (1980)].

[38]R. L. Bell, *Negative Electron Affinity Devices* (Clarendon, Oxford, 1973).

[39]A. D. Korinfskii and A. L. Musatov, Pis'ma Zh. Eksp. Teor. Fiz. **37**, 462 (1983) [JETP Lett. **37**, 547 (1983)].

[40]G. W. Gobeli, F. G. Allen, and E. O. Kane, Phys. Rev. Lett. **12**, 94 (1964).

[41]D. T. Pierce and F. Meier, Phys. Rev. B **13**, 5484 (1976).

[42]B. P. Zakharchenya, V. D. Dymnikov, I. Ya. Karlik, D. N. Mirlin, L. P. Nikitin, V. I. Perel', I. I. Reshina, and V. F. Sapega, in Proceedings of the 15th International Conference on Physics of Semiconductors, Kyoto, 1980 [J. Phys. Soc. Jpn. Suppl. A **49**, 573 (1980)].

[43]C. L. Tang and D. J. Erskine, Phys. Rev. Lett. **51**, 840 (1983).

[44]L. W. James and J. L. Moll, Phys. Rev. **183**, 740 (1969).

[45]L. W. James, Solid State Electronics Laboratory (Stanford University), Technical Report No. 5221-2, 1969 (unpublished).

[46]B. P. Zakharchenya, V. I. Zemskii, and D. N. Mirlin, Fiz. Tverd. Tela (Leningrad) **19**, 1725 (1977) [Sov. Phys.—Solid State **19**, 1006 (1977)].

[47]R. Allenspach, F. Meier, and D. Pescia, Appl. Phys. Lett. **44**, 1107 (1984).

[48]D. Pescia, M. Baumberger, and F. Meier, Solid State Commun. **50**, 417 (1984).

[49]E. O. Kane, in *Semiconductors and Semimetals,* edited by R. K. Willardson and A. C. Beer (Academic, New York, 1966), Vol. 1, Chap. III.

[50]A. I. Ekimov and V. I. Safarov, Pis'ma Zh. Eksp. Teor. Fiz. **13**, 700 (1971) [JETP Lett. **13**, 495 (1971)].

[51]R. I. Dzhioev, B. P. Zakharchenya, and V. G. Fleisher, Pis'ma Zh. Eksp. Teor. Fiz. **14**, 553 (1971) [JETP Lett. **14**, 381 (1971)].

[52]D. Z. Garbuzov, A. I. Ekimov, and V. I. Safarov, Zh. Eksp. Teor. Fiz. Pis'ma Red. **13**, 36 (1971) [JETP Lett. **13**, 24 (1971)].

[53]M. Erbudak and B. Reihl, Appl. Phys. Lett. **33**, 584 (1978).

[54]B. Reihl, M. Erbudak, and D. M. Campbell, Phys. Rev. B **19**, 6358 (1979).

[55]C. K. Sinclair, in *High Energy Physics with Polarized Beams and Polarized Targets,* edited by C. Joseph and J. Soffer (Birkhäuser, Basel, 1981), p. 27.

[56]For GaAs(110) face, spin precession in the DP field of the band-bending region has very recently been reported in the case of ballistically emitted electrons [H. Riechert, S. F. Alvarado, A. N. Titkov, and V. I. Safarov, Phys. Rev. Lett. **52**, 2297 (1984)].

[57]V. G. Fleisher, R. I. Dzhioev, B. P. Zakharchenya, and L. M. Kanskaya, Pis'ma Zh. Eksp. Teor. Fiz. **13**, 422 (1971) [JETP Lett. **13**, 299 (1971)].

[58]D. Z. Garbuzov, R. I. Dzhioev, L. M. Kanskaya, and V. G. Fleisher, Fiz. Tverd. Tela (Leningrad) **14**, 1720 (1972) [Sov. Phys. Solid State **14**, 1481 (1972)].

[59]R. Azria, P. Girard, and J. P. Ziesel (private communication).

[60]D. T. Pierce, F. Meier, and P. Zürcher, Phys. Lett. **51A**, 465 (1975).

[61]D. T. Pierce, G.-C. Wang, and R. J. Celotta, Appl. Phys. Lett. **35**, 220 (1979).

[62]C. Y. Prescott *et al.*, Phys. Lett. **84B**, 524 (1979).

[63]M. Eminyan and G. Lampel, Phys. Rev. Lett. **45**, 1171 (1980).

[64]A. B. McDonald, E. D. Earle, and E. T. H. Clifford, in *High Energy Spin Physics—1982* (Brookhaven National Labs), edited by G. M. Bunce (AIP, New York, 1982), p. 586.

[65]K. Bartschat, G. F. Hanne, and A. Wolcke, Z. Phys. A **304**, 89 (1982).

[66]M. Campagna, S. F. Alvarado, and F. Ciccacci, in *High Energy Spin Physics—1982* (Brookhaven National Labs), edited by G. M. Bunce (AIP, New York, 1982), p. 566.

[67]S. F. Alvarado, F. Ciccacci, S. Valeri, M. Campagna, R. Feder, and H. Pleyer, Z. Phys. B **44**, 259 (1981).

[68]C. Hermann, G. Lampel, H.-J. Drouhin, and D. M. Campbell, in Proceedings of the International Symposium on Polarization and Correlation in Electron-Atom Collisions, Münster, Federal Republic of Germany, 1983 (unpublished).

[69]C. S. Feigerle, D. T. Pierce, A. Seiler, and R. J. Celotta, Appl. Phys. Lett. **44**, 866 (1984).

[70]E. M. Conwell, in *High Field Transport in Semiconductors,* Suppl. 9 of *Solid State Physics,* edited by F. Seitz, D. Turnbull, and H. Ehrenreich (Academic, New York, 1957).

[71]A. Tardella (private communication).